International Journal of Informatics and Computation (IJICOM)
Vol. 8, No. 1, 2026
ISSN: 2685-8711, E-ISSN: 2714-5263 DOI: 10.35842/ijicom

Evaluation of EMA-Attention U-Net for Brain Hemorrhage Segmentation

Afu Ichsan Pradana[1], Fajar Suryani[2], Ilham Tristadika Saputra[3]

Abstract
This paper applies an enhanced multi-class segmentation approach for brain hemorrhage detection on head CT images. We address the limitation of standard architectures that struggle to delineate lesion boundaries under complex multi-class conditions, where variations in size, shape, and visual similarity are significant. We utilize an improved Attention U-Net by replacing the conventional attention mechanism with Efficient Multi-Scale Attention (EMA), aiming to strengthen feature representation while preserving the original encoder–decoder structure. We train and evaluate both the baseline and the proposed models on a head CT dataset with COCO-based annotations converted into pixel-wise masks, using metrics including Dice coefficient, Intersection over Union (IoU), precision, recall, parameter count, and inference speed. This study obtains clear performance improvements from the proposed EMA-Attention U-Net. We achieve a higher validation Dice score of 0.7836 compared to 0.7396 from the baseline. On the global macro test evaluation, we observe significant gains in Dice (0.1420 to 0.2898), IoU (0.0982 to 0.2475), and precision (0.2031 to 0.3837). Although recall slightly decreases from 0.6927 to 0.6476 and inference speed reduces from 133.12 FPS to 91.15 FPS, we maintain a nearly identical parameter count (7,791,285 to 7,794,805). These results show that we can improve spatial accuracy and segmentation consistency with minimal computational overhead, confirming that EMA is an effective attention mechanism for complex multi-class medical image segmentation.

Keywords:
Brain Hemorrhage, Segmentation, Attention U-Net, Efficient Multi-Scale Attention

1. Introduction

Brain hemorrhage is a critical neurological emergency that requires rapid and reliable assessment on head CT because treatment decisions often depend on lesion location, burden, and subtype[1], [2], [3]. In emergency practice, non-contrast CT remains the preferred first-line imaging modality because it is fast, widely available, and clinically suitable for early evaluation of acute intracranial bleeding[3],[4]. However, accurate delineation of hemorrhagic regions remains difficult. Manual annotation is time-consuming and prone to inter-observer variability, particularly when lesions are small, irregular, or poorly contrasted against surrounding tissue[5]. These limitations have encouraged the development of automatic segmentation methods for head CT analysis[6], [7], [6].

The rapid advancement of deep learning and computational intelligence has led to their widespread adoption in various complex medical and general image analysis tasks. Recent studies have demonstrated the efficacy of these approaches in diverse areas, ranging from improving hydrocephalus diagnosis and utilizing fine-tuned Convolutional Neural Networks (CNN) for brain tumor classification[8], to employing robust mobile architectures for cultural heritage motif classification[9]. These cross-domain successes highlight a fundamental

Corresponding Author: Afu Ichsan Pradana (afu_ichsan@udb.ac.id)
1 Afu Ichsan Pradana, Universitas Duta Bangsa Surakarta (afu_ichsan@udb.ac.id)
2 Fajar Suryani, Universitas Duta Bangsa Surakarta (fajar_suryani@udb.ac.id)
3 Ilham Tristadika Saputra, Universitas Duta Bangsa Surakarta (210103020@mhs.udb.ac.id)

principle: tailored architectural modifications are essential for addressing the specific challenges of complex datasets.

Recent reviews on medical image segmentation indicate that encoder-decoder architectures derived from U-Net remain among the most widely used foundations for pixel-wise medical image analysis because they preserve local detail while capturing broader contextual information[10]. In hemorrhage imaging, U-Net-based frameworks have been applied successfully to lesion delineation, quantification, and subtype-specific analysis, demonstrating that deep segmentation can support clinically meaningful assessment[9], [10] . Nevertheless, these studies also show that performance tends to degrade when lesion boundaries are indistinct, lesion sizes vary substantially, or minority classes are underrepresented [11], [12]

To address these issues, several studies have refined the U-Net family through residual design, semi-supervised learning, transformer integration, and richer feature fusion. For example, semi-supervised multi-task attention-based U-Net was used to stabilize intracranial hemorrhage subgroup segmentation[11], while MSRL-Net was proposed to improve segmentation performance for small lesion regions[12]. Transformer-assisted and residual U-Net variants have also been reported to improve feature representation for intracerebral hemorrhage segmentation[13], [14]. In parallel, attention-driven models such as attention-based residual U-Net and spatial attention-based CSR-Unet have shown that selective feature refinement can improve lesion localization and class-specific delineation[15], [16].

An additional challenge arises in full multi-class segmentation, where the model must predict all lesion-related classes within a single framework. This setting is substantially more difficult than binary segmentation because the network must separate visually similar categories while handling severe imbalance in class frequency and lesion morphology[17], [18]. Recent multiclass and multi-label studies confirm that this remains a demanding problem in head CT analysis, even when advanced U-Net-based architectures are used[18]. In other words, a conventional skip-connection refinement strategy may not be sufficient when the target includes all classes in the dataset rather than a single dominant lesion type. A relevant direction for addressing this limitation is to strengthen the feature representation itself through more expressive multi-scale attention. Recent journal studies in hemorrhage segmentation have shown that more discriminative feature modeling, including attention, dilated attention, symmetry-guided learning, and dense refinement, can improve overlap quality and robustness in difficult CT cases[19], [20], [21].

Based on this rationale, this study compares the standard Attention U-Net with an EMA-enhanced variant for full multi-class brain hemorrhage segmentation on head CT images. The contribution of this work lies in two aspects. First, it examines whether a stronger attention formulation can improve segmentation quality without changing the overall backbone structure. Second, the evaluation is conducted across all dataset classes, rather than in a binary or limited-subtype setting. By positioning the study in this way, the work aims to provide clearer evidence on how attention refinement affects multi-class hemorrhage segmentation under a realistic and clinically relevant problem setting[15].

The main contributions and novelties of this research are summarized as follows, the integration of the Efficient Multi-Scale Attention (EMA) module into the U-Net architecture. The EMA algorithm was specifically chosen due to its capability to process parallel group-based features and facilitate cross-spatial interactions. This mechanism is critical for accurately tracking micro-lesions and resolving complex boundaries that are often missed by conventional attention mechanisms. We present a comprehensive evaluation of the model in a full multi-class segmentation scenario.

2. Related Works

Automatic hemorrhage segmentation on head CT has been widely studied because manual delineation is time-consuming and subject to inter-observer variation, especially when lesions are small, irregular, or poorly contrasted. U-Net remains one of the most influential baseline models in medical image segmentation due to its encoder–decoder structure and skip connections, which preserve spatial detail while capturing contextual information[1], [6]. However, previous studies have shown that standard U-Net may struggle when lesion boundaries are unclear, lesion size varies substantially, or class imbalance is severe [11].

To address these limitations, several studies have proposed improved U-Net-based frameworks for hemorrhage segmentation. Hssayeni et al. demonstrated the feasibility of deep convolutional segmentation for intracranial hemorrhage and provided an important benchmark dataset[3]. Patel et al. extended this direction using 3D convolutional modeling for spontaneous intracerebral hemorrhage[11]. Wang et al. introduced a semi-supervised multi-task attention-based U-Net, while Wang and Wang proposed MSRL-Net to improve segmentation performance on difficult hemorrhagic regions[12], [13]. Other works further explored stronger feature extraction and multi-scale modeling, including transformer-assisted architectures and residual refinements, showing that richer representation learning can improve lesion delineation on CT[22].

Attention mechanisms have become a major extension of the U-Net family. Attention U-Net introduced attention gates to refine skip-connection features before they are fused into the decoder [23]. This idea has since been adopted in several hemorrhage segmentation studies. Recent studies reported improved intracranial hemorrhage segmentation using All Attention U-Net[15]. Lin et al. proposed an attention-based residual U-Net for multi-label brain hemorrhage segmentation, while Prakasam and Prakasam developed a spatial attention-based CSR-Unet for subdural and epidural hemorrhage segmentation and classification[17]. More recent works, such as IHA-Net and DDANet, also confirmed that attention-based feature refinement can improve the detection of small lesions and challenging boundaries[18].

Despite these advances, an important gap remains. Many previous studies focused on binary segmentation, a limited number of hemorrhage subtypes, or task-specific settings rather than full multi-class segmentation across all lesion categories[20]. Yet multiclass segmentation is substantially more difficult because the model must distinguish visually similar categories while coping with unequal class frequencies and variable lesion morphology. This creates a need for stronger feature representation, not only at the skip connection level but throughout the network.

In this context, Efficient Multi-Scale Attention (EMA) offers a relevant alternative. EMA was introduced as a lightweight attention module that combines grouped channel processing, parallel branches, and cross-spatial interaction to enhance feature representation efficiently[21] Although originally evaluated in general vision tasks, its design is suitable for semantic segmentation because it can preserve both local details and broader spatial dependencies. Therefore, replacing the conventional attention mechanism in Attention U-Net with EMA is a reasonable step for improving full multi-class hemorrhage segmentation.

3. Proposed Method

This study proposes an enhanced multi-class brain hemorrhage segmentation model by integrating Efficient Multi-Scale Attention (EMA) into the Attention U-Net framework. The main objective is to examine whether replacing the standard attention mechanism with EMA can improve segmentation performance when all hemorrhage classes in the dataset are segmented simultaneously. This design is motivated by the same problem identified in prior work, namely that strengthening feature pathways and skip-connection design is important for improving segmentation performance on complex medical images. Fig. 1. Proposed method based on EMA-Attention U-Net for multi-class brain hemorrhage segmentation. The network consists of an encoder, bottleneck, EMA-based attention refinement, and decoder. In the proposed design, EMA enhances feature maps through grouped channel interaction, parallel branches, and cross-spatial learning, followed by pixel-wise classification for all hemorrhage classes.

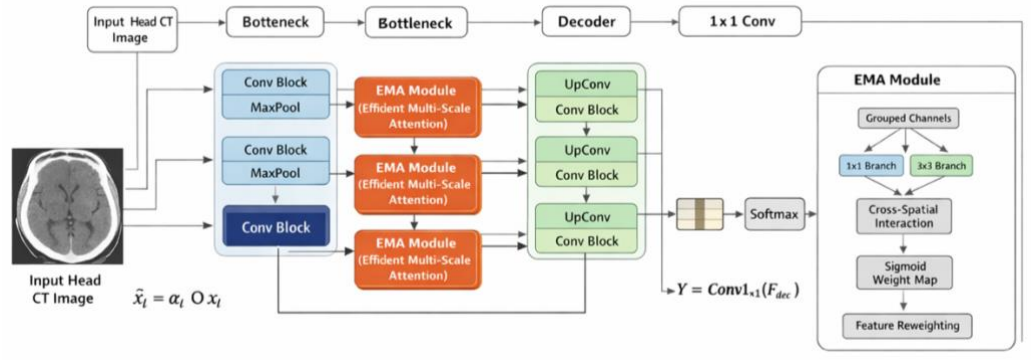

Fig. 1. Proposed Method

In this study, as the baseline model follows the standard Attention U-Net architecture. It consists of an encoder, a bottleneck layer, and a decoder. The encoder extracts hierarchical features through repeated convolutional blocks and down-sampling operations. The decoder gradually restores spatial resolution through up-sampling and feature fusion. Skip connections are used to transfer fine-grained encoder information to the decoder so that spatial details are preserved during reconstruction. In the standard Attention U-Net, each skip connection is filtered by an attention gate before fusion. Let $x_l$denote the encoder feature at level l, and let $g_l$denote the decoder gating signal. The attention gate computes a relevance map that modulates the encoder feature before concatenation. The filtered feature can be expressed as

$$\hat{x}_l = \alpha_l \odot x_l \tag{1}$$

where $\alpha_l$is the attention coefficient and $\odot$denotes element-wise multiplication. This mechanism helps suppress irrelevant background information and preserves lesion-relevant regions during decoding.

In this paper, we proposed EMA-Attention U-Net to replace the conventional attention component with the Efficient Multi-Scale Attention (EMA) module. The fundamental limitation of standard attention gates is their reliance on single-scale spatial filtering, which frequently fails to capture the intricate morphological variations of different hemorrhage subtypes. EMA overcomes this by constructing multi-scale spatial pathways, making it critically important for full multi-class segmentation where distinguishing visually overlapping classes is required.

Given an intermediate feature map $F \in \mathbb{R}^{C\times H\times W}$, EMA first divides the channels into Ggroups. In this study, the default number of groups follows the original EMA setting, namely $G = 32$, while practical adjustment is allowed when the channel dimension is not divisible by 32. The original EMA experiments also used $G = 32$as the standard configuration for fair comparisons. The grouped feature representation can be written as

$$F \to \{F_1, F_2, \dots, F_G\} \quad (2)$$

where each $F_i \in \mathbb{R}^{\frac{C}{G}\times H\times W}$ Each grouped feature is then processed by parallel transformations to obtain local and broader spatial responses. These responses are fused through cross-spatial interaction to generate refined attention weights. The refined feature for each group is obtained as

$$\tilde{F}_i = \sigma(W_i) \odot F_i \quad (3)$$

where $W_i$denotes the learned spatial weight map for the i-th group, $\sigma(\cdot)$is the sigmoid activation, and $\odot$denotes element-wise multiplication. The refined groups are finally merged back into the original feature dimension to produce the EMA-enhanced output:

$$\tilde{F} = \text{Concat}(\tilde{F}_1, \tilde{F}_2, \dots, \tilde{F}_G) \quad (4)$$

In this work, the EMA module is embedded into the attention pathway of the U-Net-based segmentation network so that feature refinement is not limited to simple gating alone. The purpose is to strengthen the representation of hemorrhagic regions with varying sizes, shapes, and class distributions before feature fusion in the decoder stage.

As output formulation for Multi-Class segmentation, the final decoder feature is projected into Koutput channels using a 1×1 convolution, where K represents the total number of segmentation classes including all hemorrhage categories and background. The final prediction is expressed as

$$Y = \text{Conv}_{1\times1}(F_{\text{dec}}) \quad (5)$$

where $F_{\text{dec}}$is the last decoder feature map. Pixel-wise class probabilities are then obtained through softmax:

$$P_c(u,v) = \frac{\exp\left(Y_c(u,v)\right)}{\sum_{k=1}^{K} \exp\left(Y_k(u,v)\right)} \quad (6)$$

where $P_c(u,v)$is the probability that pixel (u, v)belongs to class c. The predicted label of each pixel is assigned to the class with the highest probability.

4. Experimental Setup

4.1. Dataset

In this study, we conducted on a head CT hemorrhage segmentation dataset obtained from Roboflow in COCO segmentation format[24]. In the earlier baseline study, the same dataset source and annotation format were used, where each CT image was accompanied by polygon-based annotations that could be converted into pixel-wise masks for supervised segmentation. The dataset consisted of 1,995 training images, 498 validation images, and 97 test images[25]. In the present study, the task was formulated as full multi-class segmentation, meaning that all annotated hemorrhage classes in the dataset were included rather than collapsing the problem into a binary mask. The COCO annotations were converted into class-indexed pixel masks, where each pixel was assigned either to the background or to one of the hemorrhage classes.

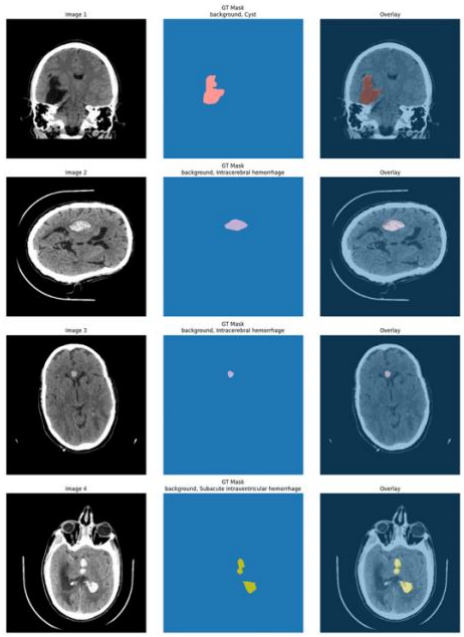

Fig. 2. Dataset preparation pipeline

Fig. 2 illustrates the dataset preparation process. It presents an example of the original head CT image, the corresponding converted segmentation mask, and the resized representation used as the final model input. The figure highlights how raw annotations are transformed into structured pixel-level labels, which serve as the ground truth during training.

4.2. Experimental Setup

All experiments were conducted on a workstation with the hardware and software environment summarized in Table 1.

Table 1. Experimental Environment

Name	Specification
CPU	Intel(R) Xeon(R) W-1390P
GPU	NVIDIA RTX A4000
VRAM	16 GB
RAM	32 GB
Python Version	3.10.12
PyTorch Version	2.6.0
Cuda Version	12.2

The models implemented Python and trained with GPU acceleration. This environment was used consistently for both the baseline and the proposed model to ensure a fair comparison.

4.3. Training and Evaluation Process

To ensure a fair comparison, both models were trained using the same data split, pre-processing pipeline, optimizer, and number of epochs.

Table 2. Training Protocol

Parameter	Setting
Task	Full multi-class brain hemorrhage segmentation
Input data format	COCO segmentation annotations converted to pixel-wise masks
Input image type	Head CT images
Input size	Fixed resized resolution
Output	Pixel-wise multi-class segmentation map
Baseline model	Standard Attention U-Net
Proposed model	EMA-Attention U-Net
Optimizer	Adam
Learning rate	1×10^{-4}
Loss function	Multi-class Cross-Entropy Loss
Batch setting	Same for both models
Number of epochs	50
Model selection	Best model based on validation performance
Evaluation metrics	Dice, IoU, Precision, Recall
Efficiency metrics	Parameter count, inference time, FPS

Table 2. summarizes the training protocol to support the model construction. Both the baseline Attention U-Net and the proposed EMA-Attention U-Net were trained under the same optimization setting to ensure a fair comparison. The models were optimized using Adam with a learning rate of $1 \times 10^{-4}$for 50 epochs. In the multi-class setting, COCO segmentation annotations were converted into pixel-wise masks, and the best model was selected based on validation performance.

5. Result and Analysis

5.1. Training Behavior

Both models converged during training, as indicated by the steady decrease in training loss and the increase in validation Dice. As shown in Fig. 3, the baseline Attention U-Net and the proposed EMA-Attention U-Net both reduced loss rapidly during the early epochs, followed by a slower and more stable convergence phase. However, the proposed model achieved a consistently higher validation Dice in the later epochs.

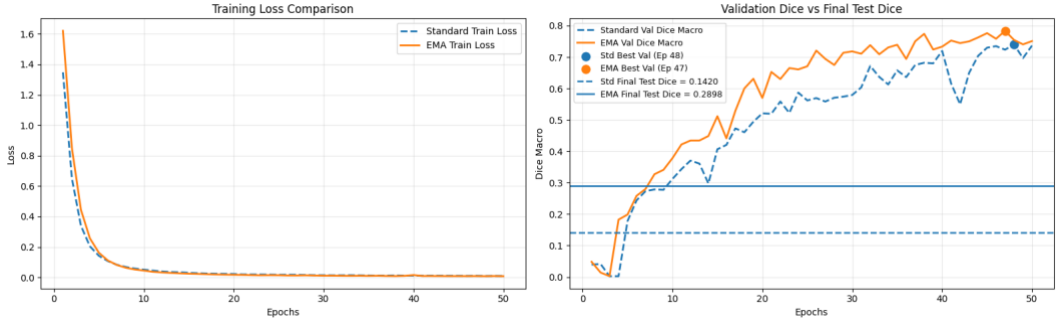

Fig. 3. Training Result

The best validation Dice of the baseline model was 0.7396 at epoch 48, whereas the EMA-Attention U-Net reached 0.7836 at epoch 47. This result indicates that the proposed attention formulation produced a stronger validation representation and reached its best performance slightly earlier. The trend in Fig. 3 also confirms that the EMA-based model maintained a more favorable validation trajectory near the end of training.

5.2. Quantitative Results

The final test results should be interpreted from two perspectives. First, using the same batch-average Dice style as in the training loop, the baseline model obtained 0.3484, while the EMA-Attention U-Net reached 0.2726. From this narrow training-style view, the baseline appeared stronger. However, the more appropriate final evaluation for the paper is the global macro test metric, computed across all classes over the full test set. Under this setting, the proposed model outperformed the baseline clearly. The baseline Attention U-Net obtained a macro-Dice of 0.1420, macro IoU of 0.0982, precision of 0.2031, and recall of 0.6927. In comparison, EMA-Attention U-Net achieved a macro Dice of 0.2898, macro IoU of 0.2475, precision of 0.3837, and recall of 0.6476. This corresponds to improvements of 104.12% in Dice, 152.07% in IoU, and 88.89% in precision, while recall decreased by 6.51%.

Table 3. Final quantitative comparison on the test set

Metric	AttUnet standar	EMA-AttUNet	Observation
Best validation Dice	0.7396	0.7836	Higher in EMA
Best validation epoch	48	47	EMA peaked earlier
Final test Dice training	0.3484	0.2726	Higher in baseline
Final test Dice global macro	0.1420	0.2898	EMA +104.12%
Final test IoU global macro	0.0982	0.2475	EMA +152.07%
Final test Precision global macro	0.2031	0.3837	EMA +88.89%
Final test Recall global macro	0.6927	0.6476	Baseline +6.51%
Parameters	7,791,285	7,794,805	EMA +3,520
Inference time (ms)	7.51	10.97	Baseline faster
FPS	133.12	91.15	Baseline faster

Table 3 showed the results of the effectiveness of the EMA-Attention U-Net. In multi-class brain hemorrhage segmentation, the primary difficulty lies in isolating specific target classes within the dataset that share highly similar visual characteristics, such as subdural versus epidural hemorrhages. The baseline Attention U-Net, which relies on a standard single-scale gating mechanism, is frequently overwhelmed by this inter-class similarity, leading to scattered false positives and a low macro precision of 0.2031. Conversely, the integration of EMA directly addresses this bottleneck. By implementing parallel multi-scale branches and cross-spatial interactions, the model continuously refines both local lesion boundaries and broader contextual surroundings. This allows the network to effectively suppress irrelevant background noise while accurately classifying complex hemorrhagic regions, ultimately driving the macro precision up to 0.3837 and delivering a 152.07% relative improvement in macro IoU. To present the results of this demonstration in a more practical context, the workflow was successfully transitioned from conceptual model development to a functional application prototyping stage.

5.3. Validation and Test Results

The training curves and final evaluation are not contradictory, because they reflect different measurements. The validation Dice shown during training is computed epoch by epoch on the validation set, whereas the final reported test metrics are computed on the test set after model selection. Therefore, the best validation Dice and final test Dice are not expected to be numerically identical.

Table 4. Consistency checks for result interpretation

Model	Best Val Epoch	Best Val Dice	Final Test Dice Train	Final Test Dice Global Macro
AttUNet standar	48	0.7396	0.3484	0.1420
EMA-AttUNet	47	0.7836	0.2726	0.2898

Table 4 displayed the EMA-based model achieved the best validation Dice during training and also delivered stronger final global macro performance on the test set. This agreement supports the conclusion that the observed improvement was not incidental, but reflected a more effective attention design for full multi-class segmentation.

5.4. Comparison of Segmentation Results

In addition to the quantitative metrics, a qualitative comparison was performed to examine how both models segmented representative hemorrhage regions. Fig. 4 presents three examples consisting of the original CT image, the ground-truth mask, the prediction from the standard Attention U-Net, and the prediction from the proposed EMA-Attention U-Net.

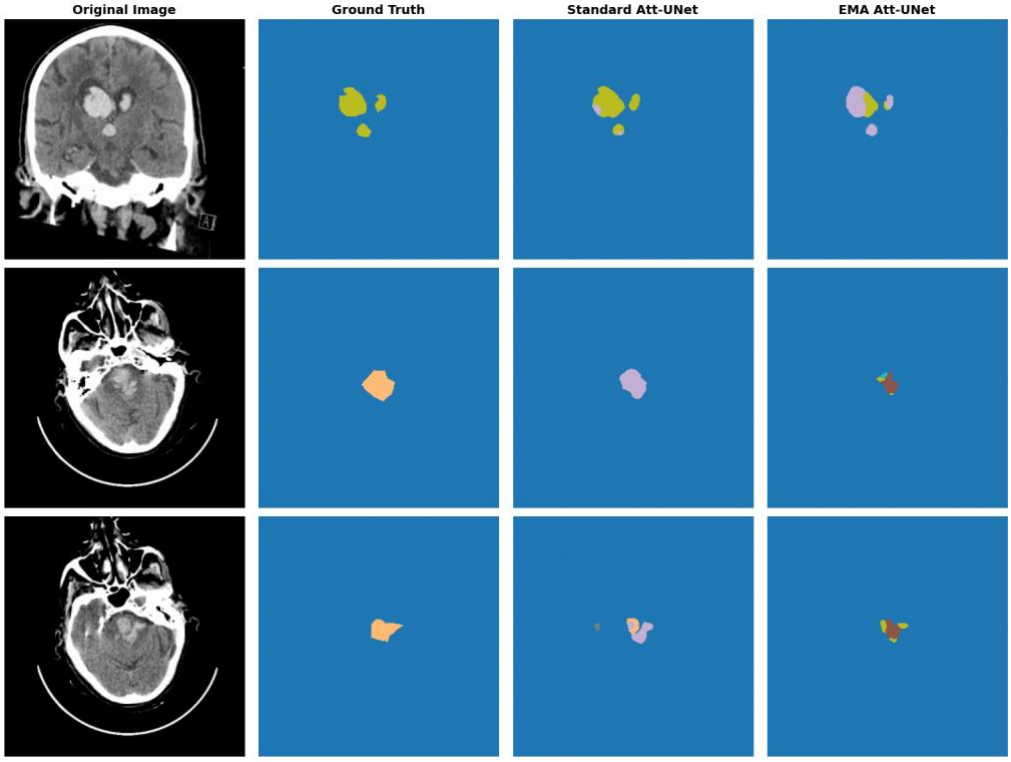

Fig. 4. Comparison of multi-class segmentation results

Therefore, the visual results show a clear difference in prediction behavior between the two models. The standard Attention U-Net tends to generate broader or less selective segmented regions, and in some cases the predicted class regions do not align well with the reference mask. By contrast, the EMA-Attention U-Net produces predictions that are generally more localized and visually closer to the annotated lesion regions. This observation is consistent with the quantitative findings, where the proposed model achieved higher Dice, IoU, and precision in the global macro evaluation.

6. Conclusion

This paper applies the EMA-Attention U-Net architecture to improve multi-class brain hemorrhage segmentation performance. We utilize the Exponential Moving Average (EMA) module to enhance feature representation and reduce false detections. The experimental results show that our approach achieves a Dice coefficient of 0.2898 and an Intersection over Union (IoU) of 0.2475, which outperform the baseline model in global macro evaluation. Although we observe a slight decrease in recall and inference speed, we confirm that the integration of EMA provides a better balance between segmentation accuracy and model efficiency. We also find that the additional parameter cost remains minimal, which makes the proposed model practical for real-world implementation.

This study applies a robust architectural enhancement to address key challenges in medical image segmentation, particularly complex lesion shape variations and severe class imbalance. We utilize the attention mechanism combined with EMA to improve the model's ability to capture subtle and irregular hemorrhage patterns. The results demonstrate that our method effectively reduces false positives and improves segmentation consistency across multiple classes. We confirm that this approach strengthens the model's generalization capability, especially in difficult cases where lesion boundaries are ambiguous and highly variable.

For future work, this paper proposes several improvements to further enhance model performance and clinical applicability. We plan to extend the current 2D framework into a 3D volumetric model to capture inter-slice spatial continuity in head CT scans. We also aim to address class imbalance more effectively by applying boundary-aware loss functions and synthetic data augmentation techniques. These strategies will help improve the representation of underrepresented hemorrhage subtypes. Overall, we expect that these enhancements will make the proposed model more reliable and suitable for broader clinical deployment.

Acknowledgment

The authors gratefully acknowledge the financial support provided by the Institute for Research and Community Service (LPPM), Universitas Duta Bangsa Surakarta, under contract number **154/UDB.LPPM/A.34-HK/IX/2025**, which enabled the successful completion of this research.

References

[1] P. Hu and Y. Zhang, "Deep learning-assisted detection and segmentation of intracranial hemorrhage in noncontrast computed tomography scans of acute stroke patients: A systematic review and meta-analysis," *Quantitative Imaging in Medicine and Surgery*, vol. 14, 2024.

[2] M. D. Hssayeni *et al.*, "Intracranial hemorrhage segmentation using a deep convolutional model," *Data*, vol. 5, no. 1, 2020, doi: 10.3390/data5010014.

[3] Patel *et al.*, "Intracerebral haemorrhage segmentation in non-contrast CT," *Scientific Reports*, vol. 9, 2019, doi: 10.1038/s41598-019-54412-7.

[4] Arab *et al.*, "A fast and fully automated deep-learning approach for accurate hemorrhage segmentation and volume quantification in non-contrast whole-head CT," *Scientific Reports*, vol. 10, 2020, doi: 10.1038/s41598-020-76459-7.

[5] N. A. M. Coorens *et al.*, "Intracerebral hemorrhage segmentation on noncontrast computed tomography using a masked loss function U-Net approach," *Journal of Computer Assisted Tomography*, vol. 47, no. 1, pp. 25–32, 2023.

[6] X. Liu *et al.*, “A review of deep-learning-based medical image segmentation: Methods and applications,” *Sustainability*, vol. 13, no. 3, 2021, doi: 10.3390/su13031224.
[7] Y. Xu *et al.*, “Advances in medical image segmentation,” *Bioengineering*, vol. 11, no. 10, 2024.
[8] J. Xu *et al.*, “Deep network for the automatic segmentation and quantification of intracranial hemorrhage on CT,” *Frontiers in Neuroscience*, vol. 15, 2021, doi: 10.3389/fnins.2021.619263.
[9] J. L. Wang *et al.*, “Segmentation of intracranial hemorrhage using semi-supervised multi-task attention-based U-Net,” *Applied Sciences*, vol. 10, no. 9, 2020, doi: 10.3390/app10093297.
[10] H. Wang and X. Wang, “MSRL-Net: An automatic segmentation of intracranial hemorrhage for CT images based on the U-Net framework,” *Applied Sciences*, vol. 13, no. 21, 2023, doi: 10.3390/app132111781.
[11] Z. Piao *et al.*, “Intracerebral hemorrhage CT scan image segmentation with HarDNet-based transformer,” *Scientific Reports*, vol. 13, 2023, doi: 10.1038/s41598-023-33775-y.
[12] Q. T. Hoang *et al.*, “An efficient CNN-based method for intracranial hemorrhage segmentation from computerized tomography imaging,” *Journal of Imaging*, vol. 10, no. 4, 2024, doi: 10.3390/jimaging10040077.
[13] P. Prakasam and S. N. Ahmed, “Spatial attention-based CSR-UNet framework for subdural and epidural hemorrhage segmentation and classification using CT images,” *BMC Medical Imaging*, vol. 24, 2024.
[14] X. Lin *et al.*, “Advanced multi-label brain hemorrhage segmentation using an attention-based residual U-Net model,” *BMC Medical Informatics and Decision Making*, vol. 25, 2025.
[15] S. N. Ahmed *et al.*, “Intracranial hemorrhage segmentation and classification framework in computed tomography images using deep learning techniques,” *Scientific Reports*, vol. 15, 2025.
[16] M. Monteiro *et al.*, “Multiclass semantic segmentation and quantification of traumatic brain injury lesions on head CT using deep learning: An algorithm development and multicentre validation study,” *The Lancet Digital Health*, vol. 2, no. 6, pp. e314–e322, 2020.
[17] H. Liu *et al.*, “DDANet: A deep dilated attention network for intracerebral haemorrhage segmentation,” *IET Systems Biology*, vol. 18, 2024.
[18] L. Li *et al.*, “Deep learning for hemorrhagic lesion detection and segmentation on brain CT images,” *IEEE Journal of Biomedical and Health Informatics*, vol. 25, no. 5, pp. 1646–1659, 2021.
[19] M. Nijiati *et al.*, “A symmetric prior knowledge-based deep learning model for intracerebral hemorrhage lesion segmentation,” *Frontiers in Physiology*, vol. 13, 2022.
[20] V. Abramova *et al.*, “Hemorrhagic stroke lesion segmentation using a 3D U-Net with squeeze-and-excitation blocks,” *Computerized Medical Imaging and Graphics*, vol. 90, 2021.
[21] Y. Ma *et al.*, “IHA-Net: An automatic segmentation framework for CT of tiny intracerebral hemorrhage based on improved attention U-Net,” *Biomedical Signal Processing and Control*, vol. 80, 2023.
[22] K. He, X. Zhang, S. Ren, and J. Sun, “Deep residual learning for image recognition,” *IEEE Conference on Computer Vision and Pattern Recognition (CVPR)*, pp. 770–778, 2016, doi: 10.1109/CVPR.2016.90.
[23] Ronneberger, P. Fischer, and T. Brox, “U-Net: Convolutional networks for biomedical image segmentation,” *Lecture Notes in Computer Science*, vol. 9351, Springer, pp. 234–241, 2015, doi: 10.1007/978-3-319-24574-4_28.
[24] F. Milletari, N. Navab, and S.-A. Ahmadi, “V-Net: Fully convolutional neural networks for volumetric medical image segmentation,” *2016 Fourth International Conference on 3D Vision (3DV)*, pp. 565–571, doi: 10.1109/3DV.2016.79.
[25] Oktay *et al.*, “Attention U-Net: Learning where to look for the pancreas,” *arXiv preprint arXiv:1804.03999*, 2018.